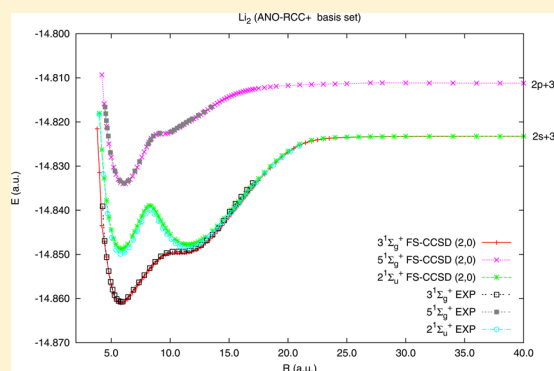


First Principle Calculations of the Potential Energy Curves for Electronic States of the Lithium Dimer

Monika Musiał* and Stanisław A. Kucharski

Institute of Chemistry, University of Silesia, Szkolna 9, 40-006 Katowice, Poland

ABSTRACT: A multireference coupled cluster (CC) approach formulated in the (2,0) sector of the Fock space (FS) is applied to study electronic states of the Li_2 molecule. The CC model including single (S) and double (D) excitations from the reference configuration is considered. The FS-CCSD(2,0) method is applicable to the description of the double electron attached states, which implies that in the neutral molecule studies the doubly ionized reference should be adopted. The results of this study include potential energy curves (PECs) and selected spectroscopic constants for 34 electronic states correlating to five lowest dissociation limits of Li_2 . Both the PECs and the computed spectroscopic constants agree very well with the experimental data wherever the latter are available. This indicates that the rigorous *ab initio* method can be successfully applied to study the energetics and molecular properties of the alkali metal diatomics.



1. INTRODUCTION

A detailed knowledge of the potential energy curves (PECs) of the alkali metal diatomics is important in the accurate evaluation of the molecular properties and correct understanding of the collision processes. Among alkali metal dimers the Li_2 system plays a special role being a second smallest homonuclear molecule, and due to that, it attracts a lot of interest both from the experimentalists and theoreticians.^{1–54} The currently available advanced spectroscopic techniques such as OODR (optical–optical double resonance),^{1–21} AOTR (all optical triple resonance),²² or CIF (collisionally induced fluorescence)^{23–26} allow for the precise measurement and the accurate spectroscopic characteristics of electronic states of Li_2 .^{1–39} On the other hand, there exist a number of papers devoted to the theoretical studies of potential energy curves and spectroscopic properties of the lithium dimer.^{39–54} Some of them^{40–44} are based on the full configuration interaction (FCI) scheme applied to two valence electrons. Since the freezing of four 1s electrons introduces a non-negligible error in the calculations the inner shells are replaced with the model or effective potential,^{40–44,55,56} which requires considering a number of additional parameters representing the inner electrons potential. Another advantage of the FCI scheme is its invariance with respect to the unitary transformation among orbitals. Hence, the inadequacies in the reference function that might occur at large distances when the closed shell molecule dissociates into the open shell fragments does not affect the FCI results. Thus, in the all electron calculations, the principal problem in the calculation of the PECs at large internuclear distances is an incorrect description of the reference function, in particular when the RHF (restricted Hartree–Fock) orbitals are used.

In the present work, we propose to study PECs of the Li_2 molecule by using a rigorous *ab initio* method based on the

multireference (MR) coupled cluster (CC) scheme^{57,58} known under acronym FS-CCSD(2,0).⁵⁹ This particular realization of the MRCC approach, based on the (2,0) sector of the Fock space (FS),⁵⁹ is designed to provide a correct and accurate description of the double electron attached (DEA) states. In other words, once the reference (RHF) function for the system A is found we may generate the accurate wave function for the system A^{-2} , or starting with the reference for the A^{+2} ion, the FS-CCSD(2,0) scheme will provide an adequate description of the neutral A molecule. The latter observation turns out to be very useful in the calculation of the PECs connected with the dissociation of the single bond. For example, the closed shell Li_2^{+2} ion dissociates into Li^+ ions which are also the closed shell units isoelectronic with the Helium atom. Hence, we may ensure the correct RHF function for the Li_2^{+2} system at any internuclear distance. By doing the FS-CCSD(2,0) calculations, we obtain the correct electronic states for the neutral Li_2 system. We see the FS-CCSD(2,0) is able to provide a description of the alkali metal dimer at any distance free of the well-known bond breaking problems.

The CC based approach ensures also another vital feature of the theoretical treatment, namely the size-extensivity, which is of particular importance in the calculations of the potential energy curves. We emphasize that these are strict *first principle* calculations without any model or effective potential parameters. In our initial studies done for the modest basis sets, we found this approach very promising for the alkali diatomics.^{48,59,60} The current work is aimed at the possible accurate description of the potential energy curves for large number of electronic states (34) for Li_2 molecule.

Received: December 12, 2013

Published: February 4, 2014

2. SYNOPSIS OF THE THEORY

In this section, we give a short description of the theory just to introduce the quantities needed to specify in an unambiguous way the applied variant of the computational scheme. The detailed description of the Fock space multireference coupled cluster scheme applicable to the double electron attached states is given elsewhere.⁵⁹ The principal idea of the MR approaches is to replace the Schrödinger equation

$$H\Psi = E\Psi \quad (1)$$

where Ψ is an exact wave function defined within the full configurational space, with the equation

$$H_{\text{eff}}\Psi_0 = E\Psi_0 \quad (2)$$

H_{eff} is an effective Hamiltonian defined within a model space \mathcal{M} , which is a low-dimension subspace of the original configurational space. Note that in both equations the eigenvalue E corresponds to the exact energy of the system. In the multireference formalism, the replacement of the exact Hamiltonian with its effective counterpart does not introduce any approximation to the energy of the system.

Within the Fock space framework, the model space \mathcal{M} is defined by the pair of integers (k, l) where k (l) is a maximum number of particles (holes) created within the valence levels. Thus, the model space in the FS-MR formalism is the configurational subspace of the Fock space obtained as a direct sum of the particular sectors $\tilde{\mathcal{M}}^{(i,j)}$

$$\mathcal{M}^{(k,l)} = \bigoplus_{i,j=0}^{i=k, j=l} \tilde{\mathcal{M}}^{(i,j)} \quad (3)$$

The sector $\tilde{\mathcal{M}}^{(i,j)}$ is d by the creation of the i particles and j holes within the m valence levels. The double electron attached states correspond to the $(2,0)$ sector, and we may write

$$\mathcal{M}^{(2,0)} = \bigoplus_{i=0}^{i=2} \tilde{\mathcal{M}}^{(i,0)} \quad (4)$$

Thus, for the m valence levels the $\mathcal{M}^{(2,0)}$ model space will include one Φ_0 configuration in the $(0,0)$ sector, m Φ^α configurations in the $(1,0)$ sector, obtained by creation of the electron in the level α , and m^2 $\Phi^{\alpha\beta}$ configurations in the $(2,0)$ sector obtained by creation of two electrons in the levels α and β .

A general expression for the H_{eff} operator for the $(2,0)$ sector can be written out as

$$H_{\text{eff}} = P^{(2,0)} H e^{S^{(0,0)} + S^{(1,0)} + S^{(2,0)}} P^{(2,0)} \quad (5)$$

where the projection operator $P^{(2,0)}$ is defined as

$$P^{(2,0)} = \sum_{\alpha\beta} |\Phi^{\alpha\beta}\rangle \langle \Phi^{\alpha\beta}| \quad (6)$$

The cluster operators in the particular sectors within the singles and doubles model are defined as

$$S^{(0,0)} = \sum_{ia} s_i^a a^\dagger i + \frac{1}{4} \sum_{abij} s_{ij}^{ab} a^\dagger b^\dagger ji \quad (7)$$

$$S^{(1,0)} = \sum_{\alpha\alpha} s_\alpha^{\bar{a}} a^\dagger \alpha + \frac{1}{2} \sum_{a\alpha bi} s_{ai}^{ab} a^\dagger b^\dagger i\alpha \quad (8)$$

$$S^{(2,0)} = \sum_{\bar{a}\bar{b}\alpha\beta} s_{\alpha\beta}^{ab} a^\dagger b^\dagger \beta\alpha \quad (9)$$

Note that we adopted a convention that the indices a, b, \dots (i, j, \dots) refer to virtual (occupied) one-particle levels while α, β, \dots refer to active particles, and \bar{a}, \bar{b}, \dots refer to inactive particles, and the prime in eq 9 indicates that the excitations within the model space are excluded.

Solutions of the MR Fock space equations are obtained in the hierarchical manner; that is, in order to solve the eigenproblem for the sector (k, l) , the solutions for all the sectors (i, j) with $i \leq k$ and $j \leq l$ are required. For the current case, it means that in order to obtain the energies and amplitudes for the $(2,0)$ sector we need to solve the $(0,0)$ and $(1,0)$ sectors. Solving the CC equations for the $(0,0)$ sector is in fact a single reference problem for the reference function Φ_0 and the operators $S_1 (\equiv T_1)$, $S_2 (\equiv T_2)$ enter the CC equations for higher sectors via \bar{H} operator, defined as $\bar{H} = e^{-T_1-T_2} H e^{T_1+T_2}$. In the current calculations the reference function Φ_0 is the RHF solution for the Li_2^{2+} ion. As it has been mentioned in the introduction, this is a closed shell molecule dissociating into the closed shell fragments, Li^+ , isoelectronic with the Helium atom, which ensures correct form of the reference RHF function in the whole range of interatomic distances.

The amplitudes $S^{(1,0)}$ and $S^{(2,0)}$ for the $(1,0)$ sector can be obtained by solving the respective FS-MRCC^{61,62} equations, but the same result can be obtained with the EA-EOMCC method, that is, the EOM (equation-of-motion) scheme applied to the single electron attached (EA) states.^{63,64} We know that the energy values obtained with the EA-EOMCC scheme are identical to those of the FS-MRCC for the $(1,0)$ sector while the corresponding eigenvectors differ only by a straightforward transformation. Once the S amplitudes for the $(0,0)$ and $(1,0)$ sectors are found, we can establish equations for the $S^{(2,0)}$ amplitudes, which subsequently are used to construct the H_{eff} operator the diagonalization of which provides the sought energies of the double electron attached states. In order to avoid convergence problems in the $(2,0)$ sector, we applied intermediate Hamiltonian (IH) strategy described in detail in our paper devoted to the FS-CCSD(2,0) method.⁵⁹

3. RESULTS AND DISCUSSION

All calculations are done using the ACES II⁶⁵ program system supplemented with the FS-CCSD(2,0) module.⁵⁹ The uncontracted ANO-RCC⁶⁶ basis set with additional two diffuse functions for s, p, d, f shells with exponents: 0.00275 and 0.000962 for s ; 0.00172 and 0.000603 for p ; 0.00675 and 0.00236 for d ; 0.01536 and 0.006144 for f (denoted as ANO-RCC+) is used. All electrons are correlated. The results are collected in Figures 1–11 and in Tables 1–7 along with the available experimental data. The size of the active space for the FS-CCSD(2,0) calculations has been set to $m = 86$ (i.e., 86 lowest virtual orbitals have been selected as active). The resulting size of the model space in the $(2,0)$ sector (m^2) is equal to 7396. The further increase in the size of the active/model space does not affect meaningfully the results. In the current calculations the orbitals used in the FS part are obtained by the RHF solution for the Li_2^{2+} system in accordance with the overall computational strategy presented in the introduction.

In Table 1, we list the calculated and experimental values of the atomic excitation energies for the Li atom. The six lowest lying states are included. In all cases, we observe an excellent agreement between computed and experimental values with the differences below 0.01 eV and the mean absolute error of 0.0025 eV. Note that the method used in the atomic calculations is fully compatible with that used in the dimer studies. The

Table 1. Excitation Energies (eV) for the Li Atom in ANO-RCC+ Basis Set

sym.	EA-EOM-CCSD (\equiv FS-CCSD(1,0))	Δ	expt. ^a
$2p^0$	1.8492	0.0014	1.8478
$2S$	3.3707	−0.0024	3.3731
$2p^0$	3.8339	−0.0004	3.8343
$2D$	3.8757	−0.0029	3.8786
$2S$	4.3400	−0.0009	4.3409
$2p^0$	4.5286	0.0070	4.5216
MAE ^b		0.0025	

^aRef 69. ^bMean absolute error.

electronic states of the open shell Li atom were studied with the Fock space scheme formulated in the (1,0) sector. This means that the reference function was obtained for the Li⁺ closed shell ion and the electron attached states resulted from the EA calculations (in fact the actual calculations were done using equivalent EA-EOMCC scheme). In Table 2, we illustrate the size-extensivity feature of the FS-CCSD(2,0) method, which tells us that the excitation energy computed for Li₂ at large *R* should be equal to the excitation energy of the Li atom or (in the case of 2p + 2p asymptote) to the sum of excitations in the two Li atoms.

The main body of the results refer to the electronic states of the Li₂ molecule. We consider in our treatment 34 states, that is, those correlating to the following dissociation limits: 2s + 2s (two states), 2s + 2p (eight states), 2s + 3s (four states), 2p + 2p (twelve states), and 2s + 3p (eight states). In the next section, we discuss the computed PECs for all studied states.

4. POTENTIAL ENERGY CURVES FOR ELECTRONIC STATES OF THE Li₂ MOLECULE

To get an idea about the positioning and mutual interrelations of the curves, we collect in Figure 1 the PECs for all 34 electronic states considered in the present work. They are naturally divided into five groups depending on the dissociation limit. Due to the specific feature of the applied computational method which uses as the reference the closed shell configurations the calculations can be done equally easy for any internuclear distance. The size-extensivity property of the FS-CC approaches ensures a rigorous agreement of the asymptotic energy values for the Li₂ system with the sum of the atomic excitation energies, see Table 2. It is also clearly seen from Figure 1 that our method provides identically the same asymptotic energy value for all states correlating to the same limit.

In Figure 2, we present the PECs that correlate to the 2s + 2s dissociation limit. The bottom $1^1\Sigma_g^+$ curve, representing the ground state, has been studied in several works.^{40–48} It shows a regular Morse-type potential with the relatively deep minimum. The theoretical curve coincides with the experimental (RKR, Rydberg–Klein–Rees) one²⁷ in the whole range where the

experimental points are available. The $1^3\Sigma_u^+$ PEC corresponding to the lowest triplet state looks at first sight as repulsive; however, the closer analysis indicates the existence of the shallow well 334 cm^{−1} deep confirmed experimentally ($D_e^{\text{exp}} = 333 \text{ cm}^{-1}$). A comparison of the calculated curve with its experimental (RKR) counterpart¹¹ shows an excellent agreement: both curves overlap in the whole range of available points, see Figure 2.

In Figure 3, we display five PECs of the $1^1\Sigma_g^+$ symmetry correlating to the asymptotes: 2s + 2p ($2^1\Sigma_g^+$), 2s + 3s ($3^1\Sigma_g^+$), 2p + 2p ($4^1\Sigma_g^+$ and $5^1\Sigma_g^+$) and 2s + 3p ($6^1\Sigma_g^+$). The $2^1\Sigma_g^+$ state is energetically separated from the remaining four, and due to that, it is the least perturbed by other states. The higher lying curves manifest more complicated shapes with shelves, which upon more detailed investigation turn out to be a second minimum. In all cases, the first minimum is relatively deep, occurring between 3.0 and 3.7 Å. The unusual shapes of the curves are caused by avoided crossing (AC), which can be observed in several cases. For example, the $3^1\Sigma_g^+$ and $4^1\Sigma_g^+$ change their shapes due to AC around 20 au. Similarly the AC involving $4^1\Sigma_g^+$ and $5^1\Sigma_g^+$ states occurs at ca. 12 au and that concerning the $5^1\Sigma_g^+$ and $6^1\Sigma_g^+$ at ca. 25 au. The depths and positions of the minima are discussed in the next section. For all states displayed in Figure 3, the experimental curves are available ($2^1\Sigma_g^+$, $3^1\Sigma_g^+$, $4^1\Sigma_g^+$, $5^1\Sigma_g^+$ and $6^1\Sigma_g^+$), and they are also plotted in the Figure 3. As we can see, they match very well the theoretical results.

In Figure 4, we show the three curves corresponding to the states of $3^3\Sigma_g^+$ symmetry. The first two curves, $1^3\Sigma_g^+$ and $2^3\Sigma_g^+$, correlating to the 2s + 2p and 2s + 3s asymptotes, respectively, manifest regular Morse-like shapes, whereas the $3^3\Sigma_g^+$ curve reveals double-well character due to avoided crossing with the $4^3\Sigma_g^+$ curve. Note that the positions of the minima are very close in all three states occurring around 5.8 au. For all theoretical curves, we were able to find their experimental analogues (^{6,7,23} for the $1^3\Sigma_g^+$, $2^3\Sigma_g^+$, and $3^3\Sigma_g^+$, respectively), and similarly, as in previous cases, the agreement between theory and experiment is excellent.

The three curves displayed in Figure 5 correspond to the $1^1\Sigma_u^+$ states. Both upper curves have a clearly outlined double-well profile. The $2^1\Sigma_u^+$ belongs to the most often studied electronic state of the lithium dimer due to the two distinct minima with relatively high barrier separating them. We observe that the shapes of the $2^1\Sigma_u^+$ and $3^1\Sigma_u^+$ curves are determined by avoided crossing. For the $1^1\Sigma_u^+$ and $2^1\Sigma_u^+$ curves, we have an access to the experimental RKR and IPA (Inverted Perturbation Approach) data,^{22,29} which are also displayed in Figure 5 and (as we can see) they fully coincide with the theoretical curves.

The potential energy curves corresponding to the $3^3\Sigma_u^+$ states are displayed in Figure 6. A strong interaction between $2^3\Sigma_u^+$ (2s + 2p asymptote) and $3^3\Sigma_u^+$ (2s + 3s asymptote) states and the resulting avoided crossing makes the $4^3\Sigma_u^+$ curve almost repulsive with a shallow well at *R* = 6.05 au. The other curve

Table 2. Li₂ Ground and Excited State Energies for Separated Atoms in ANO-RCC+ Basis Set^a

	Li	Li + Li	Li ₂ (<i>R</i> = 10000 Å)
dissociation limit	FS-CCSD(1,0)	FS-CCSD(1,0)	FS-CCSD(2,0)
2s + 2s ^b	−7.47355273 au	−14.94710546 au	−14.94710546 au
2s + 2p	1.84916574 eV	1.84916574 eV	1.84916574 eV
2s + 3s	3.37065338 eV	3.37065338 eV	3.37065338 eV
2p + 2p	2 × 1.84916574 eV	3.69833148 eV	3.69833148 eV
2s + 3p	3.83389013 eV	3.83389013 eV	3.83389013 eV

^aExcitation energies in eV. ^bTotal ground state (2s + 2s) energy in a.u.

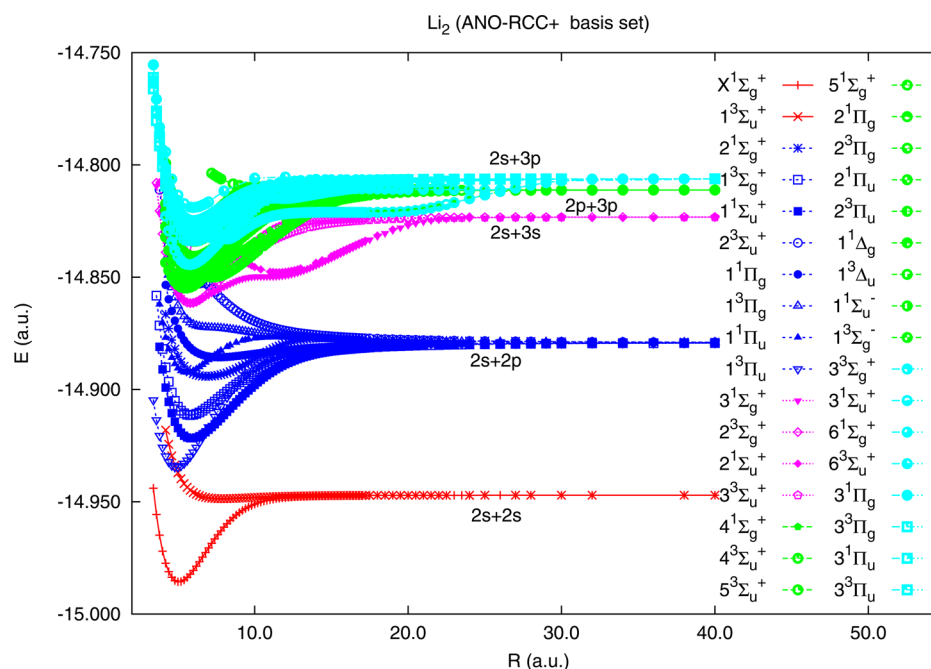


Figure 1. Potential energy curves for the ground and excited states of the Li_2 molecule with the FS-CCSD(2,0) method for $\text{Li}(2s) + \text{Li}(2s)$, $\text{Li}(2s) + \text{Li}(2p)$, $\text{Li}(2s) + \text{Li}(3s)$, $\text{Li}(2p) + \text{Li}(2p)$, and $\text{Li}(2s) + \text{Li}(3p)$ dissociation limits in the ANO-RCC+ basis set.

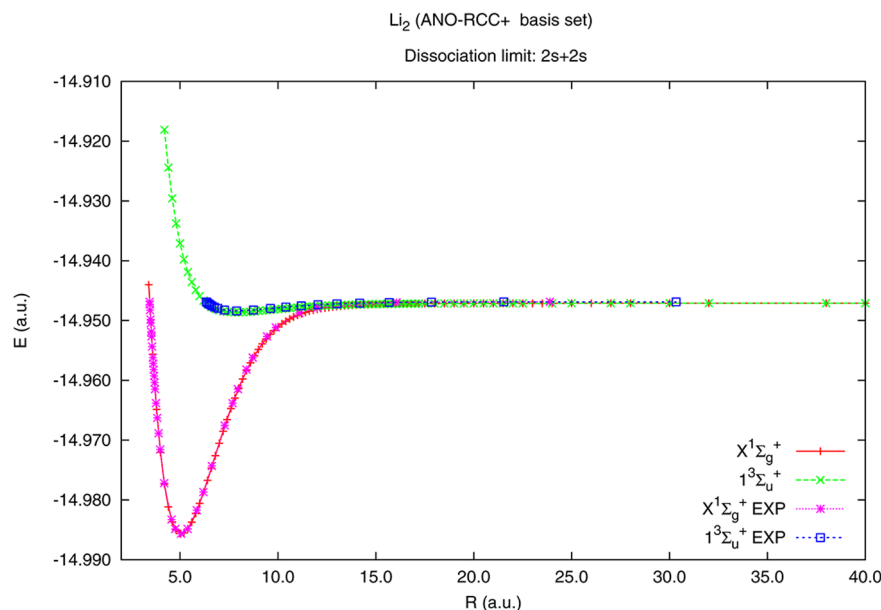


Figure 2. Potential energy curves for the Li_2 molecule with the FS-CCSD(2,0) method for $\text{Li}(2s) + \text{Li}(2s)$ dissociation limit in the ANO-RCC+ basis set. Experimental curves from refs 11 and 27.

has a minimum with large curvature resulting in the harmonic frequency larger than 350 wavenumbers. In the upper curves, we also observe ACs involving, for example, $5^3\Sigma_u^+$ ($2p + 2p$) and $6^3\Sigma_u^+$ ($2s + 3p$) curves (ca. 9 au), $4^3\Sigma_u^+$ ($2p + 2p$) and $6^3\Sigma_u^+$ (19–20 au).

The PECs corresponding to Π_g states are displayed in Figure 7 (singlets) and Figure 8 (triplets). The shallow well in the $1^1\Pi_g$ curve occurs at 7.7 au with depth of 1426 cm^{-1} (experimental value⁹ equal to 1423 cm^{-1}). The RKR data⁹ plotted in the Figure clearly support the theoretical findings. The same is true for the $2^1\Pi_g$ curves; that is, the theoretical curve overlaps nicely with the RKR one.¹⁰ The lowest triplet Π_g curve is repulsive, see Figure 8. The upper triplet curves are of regular Morse-type shape. The

$3^3\Pi_g$ curve is of double-well character with the second minimum of depth of several wavenumbers only. The experimental RKR data⁷ are available only for the $2^3\Pi_g$ state and both curves overlap.

The potential curves for the Π_u states are presented in Figures 9 and 10 for singlet and triplet states, respectively. The experimental IPA curves are available only for the singlet states: $1^1\Pi_u$ ²⁸ and $2^1\Pi_u$ ²⁹ correlating to the $2p + 2p$ and $2s + 3p$ asymptotes, respectively. In both cases, we observe an excellent agreement with our calculations, cf. Figure 9. Two of the three PECs displayed in Figure 10, $2^3\Pi_u$ and $3^3\Pi_u$ ($2p + 2p$ and $2s + 3p$ asymptotes, respectively) show some deviations from the regular Morse-type profile. This fact could be caused by the avoided

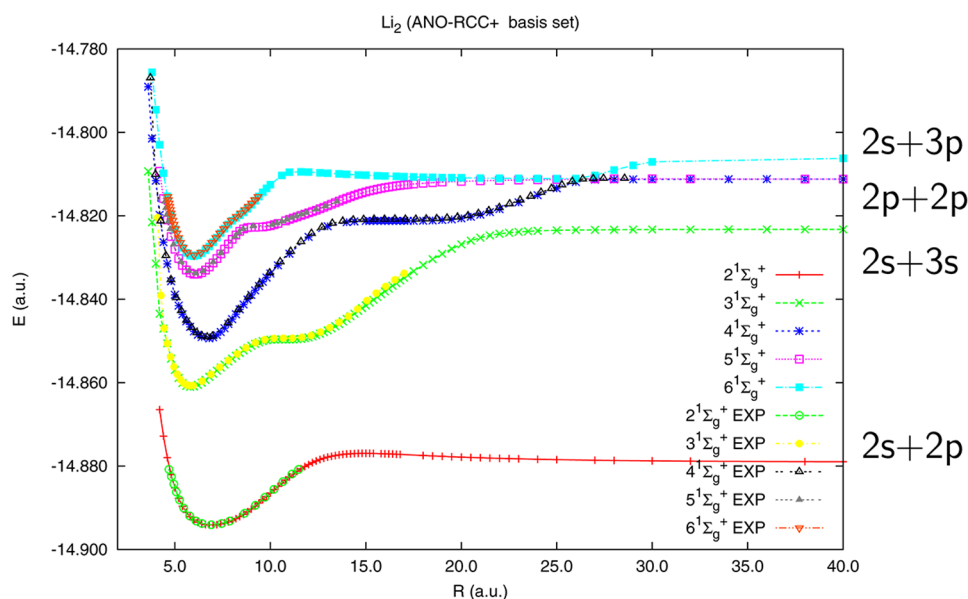


Figure 3. Potential energy curves for the Li_2 molecule with the FS-CCSD(2,0) method for the $1\Sigma_g^+$ states in the ANO-RCC+ basis set. Experimental curves from refs 1 and 3–5.

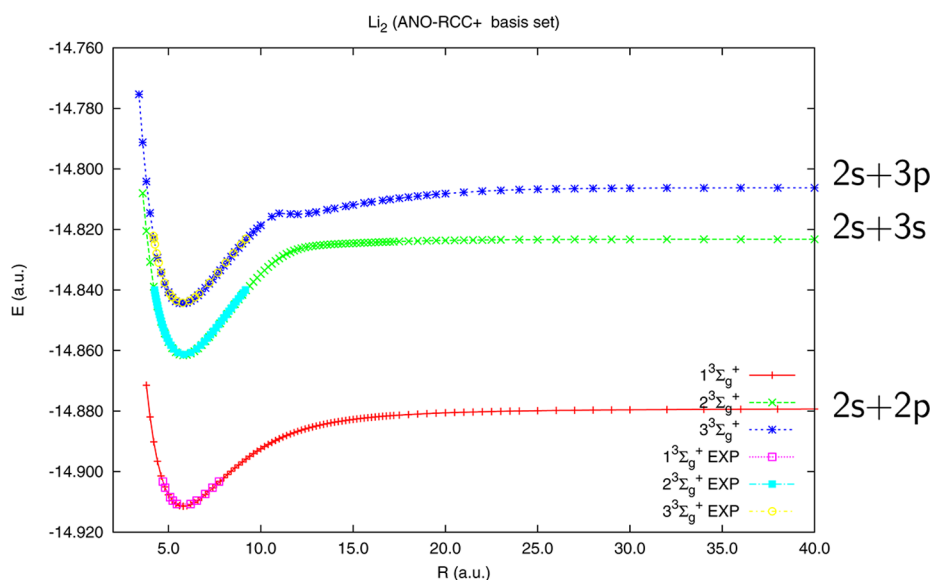


Figure 4. Potential energy curves for the Li_2 molecule with the FS-CCSD(2,0) method for the $3\Sigma_g^+$ states in the ANO-RCC+ basis set. Experimental curves from refs 6, 7, and 23.

crossings at $R \approx 8$ and 17 au. No experimental curves available for that symmetry.

The 30 curves displayed in Figures 2–10 represent eight symmetry types. The additional four curves correlating to the $2p + 2p$ asymptote are shown in Figure 11. We have here two Δ states: $1^1\Delta_g$ and $1^3\Delta_u$ and two Σ^- ones: $1^1\Sigma_u^-$ and $1^3\Sigma_g^-$. Figure 11 shows that the most stable is $1^1\Delta_g$ state with deep minimum of nearly $10\,000\text{ cm}^{-1}$, whereas the $1^1\Sigma_u^-$ state is practically repulsive. A closer analysis shows, however, a very shallow minimum 14 cm^{-1} deep occurring at ca. 14.5 au. The experimental data are available only for the $1^3\Sigma_g^-$ state,⁸ and as it can be seen in Figure 11, the two curves agree very well.

4.1. Spectroscopic Constants. In the following tables, we listed the main spectroscopic constants (with the help of the LEVEL-8 program of LeRoy⁶⁷), that is, R_e (equilibrium bond length), D_e (dissociation energy), ω_e (harmonic frequency), and

T_e (adiabatic excitation energy) for all considered states. They are grouped in five tables (Tables 3–7) depending on the dissociation limit. We compare our results with the experimental values (if the latter are available) and with the other theoretical works. Out of several papers dealing with the theoretical treatment of the electronic states of the Li_2 molecule most are focused on one or several electronic states. For comparison with our results we selected two works: one by Jasik and Sienkiewicz⁴⁰ (denoted in the tables as JS) and the other by Poteau and Spiegelmann⁴¹ (referred to as PS). These papers provide a characteristics for the number of excited states comparable with the present work. In addition, the results presented there are of high quality, and we can confront our rigorous *ab initio* results with those based on the effective potential.

In Table 3, we display the constants for the two states dissociating into $2s + 2s$ limit, that is, $1^3\Sigma_g^+$ and $1^3\Sigma_u^+$. The

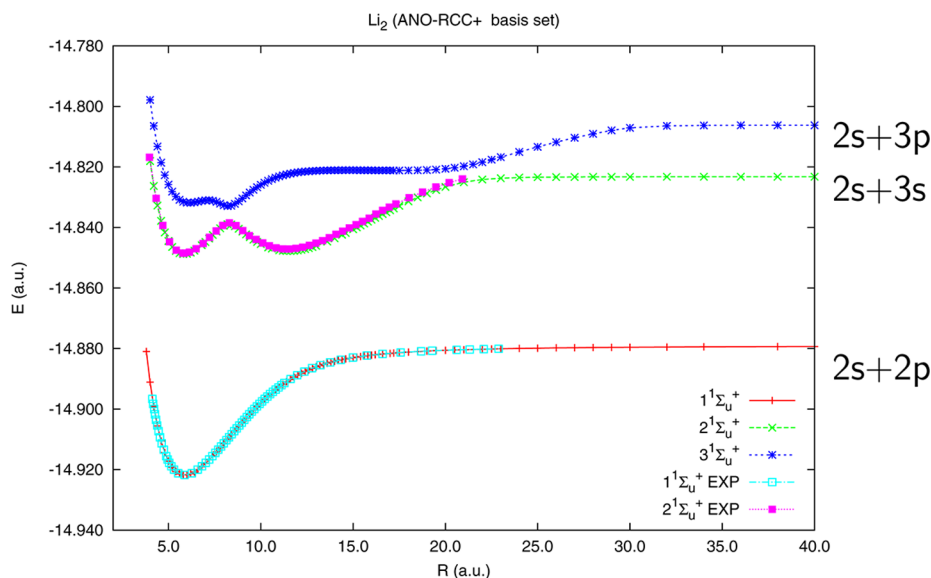


Figure 5. Potential energy curves for the Li_2 molecule with the FS-CCSD(2,0) method for the $1\Sigma_u^+$ states in the ANO-RCC+ basis set. Experimental curve from refs 22 and 29.

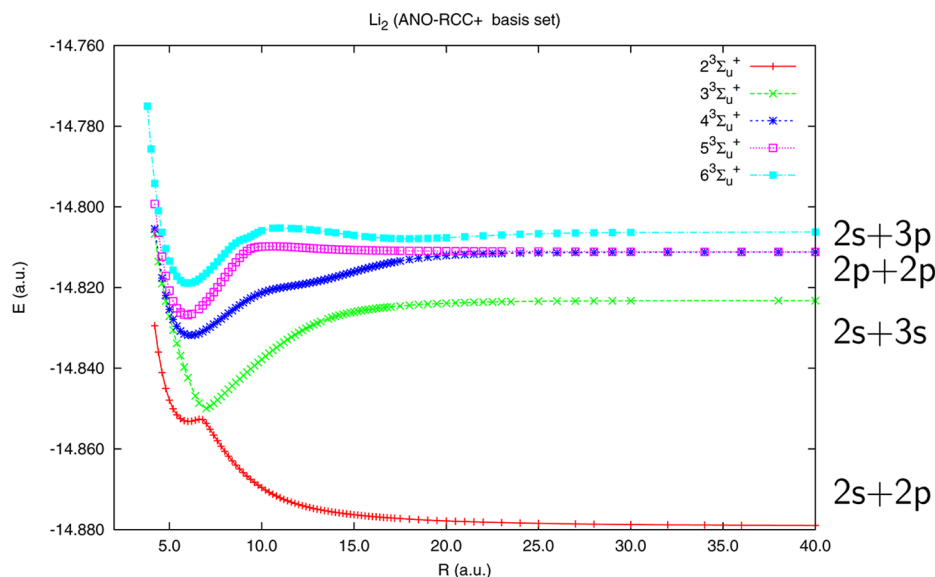


Figure 6. Potential energy curves for the Li_2 molecule with the FS-CCSD(2,0) method for the $3\Sigma_u^+$ states in the ANO-RCC+ basis set.

experimental bond length of 2.673 Å for the ground state curve differs by 0.004 Å from the computed equilibrium distance which is a better result than that obtained in other theoretical works^{40,41} with the deviations of 0.013–0.015 Å. The harmonic frequency is reproduced in our work with accuracy better than 1 cm^{-1} . The dissociation energy is off by 51 cm^{-1} , which is slightly worse result than that by PS.⁴¹ The $1^3\Sigma_u^+$ curve shows a shallow well 334 cm^{-1} deep, occurring at the bond length of 4.169 Å with the harmonic frequency of 65 cm^{-1} . These values remain in excellent agreement with the experiment with errors of 1 cm^{-1} for D_e and 0.002 Å for R_e . The adiabatic excitation energy is reproduced with an accuracy of 0.006 eV.

The results for the states correlating to the $2s + 2p$ dissociation limit are collected in Table 4. The computed equilibrium bond lengths are off by 0.002 to 0.006 Å while the harmonic frequencies are either right at the experimental values or off by up to 2 cm^{-1} . The dissociation energy in two cases ($1^1\Sigma_u^+$, $1^1\Pi_g$) is off by 3 wavenumbers, in other four ($1^3\Pi_u$, $1^3\Sigma_g^+$, $1^1\Pi_u$, $2^1\Sigma_g^+$) by

21, 12, 54, and 30 wavenumbers, respectively. This is an excellent result, remarkably better than that obtained in the other theoretical works.^{40,41} It is revealed, for example, in the values of MAE given at the bottom of Table 4, which for the present work are significantly lower than for the other computations, cf. the MAE for R_e equal to 0.004 Å vs 0.010 Å by JS and PS and for D_e : 21 cm^{-1} vs 79 cm^{-1} (JS) and 107 cm^{-1} (PS). The same pertains to the excitation energy values, T_e , obtained in this work and given in the last column of Table 4, for which the average deviation from the experiment is equal to 0.003 eV.

The four states, $3^1\Sigma_g^+$, $2^3\Sigma_g^+$, $2^1\Sigma_u^+$, and $3^3\Sigma_u^+$, belong to the group correlating to the $2s + 3s$ dissociation limit, and the respective molecular parameters are listed in Table 5. Only for three of them are the experimental data available, and on that basis, we can assess the quality of theoretical results. The computed equilibrium bond lengths are as usual very close to the observed values with the errors of 0.003 ($3^1\Sigma_g^+$), 0.001 ($2^1\Sigma_u^+$), and 0.004 Å ($2^3\Sigma_g^+$). The error in the harmonic frequency

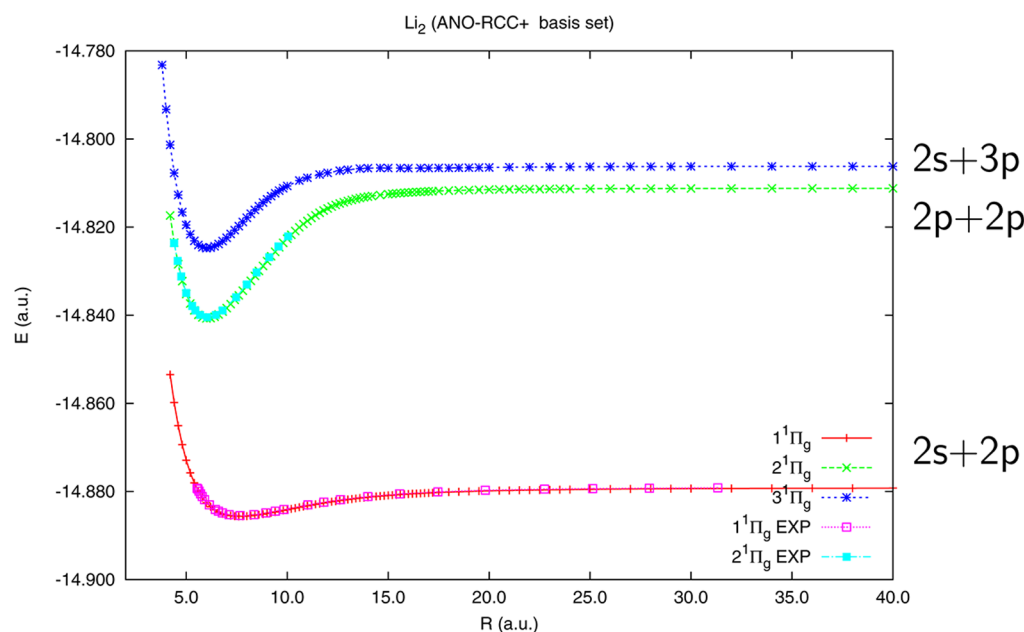


Figure 7. Potential energy curves for the Li_2 molecule with the FS-CCSD(2,0) method for the $1\Pi_g$ states in the ANO-RCC+ basis set. Experimental curves from refs 9 and 10.

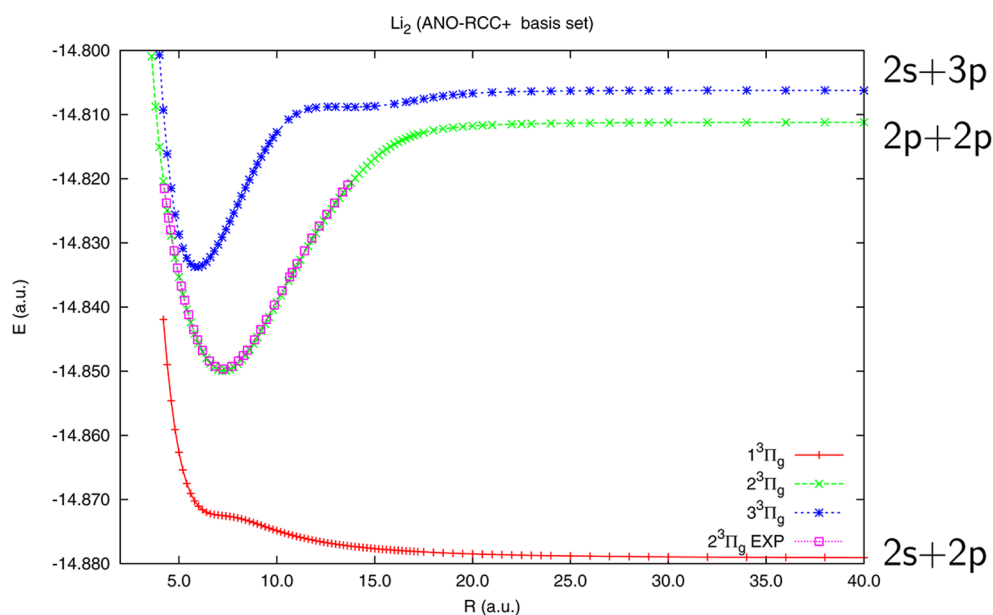


Figure 8. Potential energy curves for the Li_2 molecule with the FS-CCSD(2,0) method for the $3\Pi_g$ states in the ANO-RCC+ basis set. Experimental curve from ref 7.

calculations is in one case equal to 2 cm^{-1} and in the remaining two cases is lower than 1 cm^{-1} . The experimental data for the D_e are available only for two states ($3^1\Sigma_g^+$, $2^1\Sigma_u^+$), and the results of the current work match them very well (23 and 7 wavenumbers difference). A similar observation is true for the adiabatic excitation energy values with the errors of 0.006, 0.006, and 0.007 eV for the states: $3^1\Sigma_g^+$, $2^3\Sigma_g^+$, and $2^1\Sigma_u^+$, respectively. We observe also a good agreement with the experimental parameters relating to the second minimum of the $2^1\Sigma_u^+$ state. The computed R_e is off by 0.048 \AA and the D_e is off by 68 cm^{-1} . The experimental harmonic frequency is missing, but our value of 118 cm^{-1} remains in a good agreement with those by JS (119 cm^{-1})⁴⁰ and PS (117 cm^{-1}).⁴¹ The same is true for the T_e value with the error of 0.017 eV . Note that our calculations indicate a

presence of the second well also for the $3^1\Sigma_g^+$ state, which occurs at the $R = 5.740\text{ \AA}$. This observation has been recently confirmed experimentally,³ the other theoretical work in which the second minimum for the $3^1\Sigma_g^+$ state was observed is that by Konowalov and Fish.⁴²

The group correlating to $2p + 2p$ limit consists of 12 states and the respective molecular constants are listed in Table 6. The experimental data are available only for several of them and for those the current results are in excellent agreement. For example, for the $4^1\Sigma_g^+$ and $2^1\Pi_g$ states the equilibrium bond lengths are accurate up to 0.001 \AA ; for the $2^1\Pi_u$ the error is equal to 0.005 \AA . The largest deviation from the experiment occurs for the $2^3\Pi_g$ state for which the value obtained in the current work is equal to 3.851 \AA , that is, larger by 0.035 \AA from the experiment. We

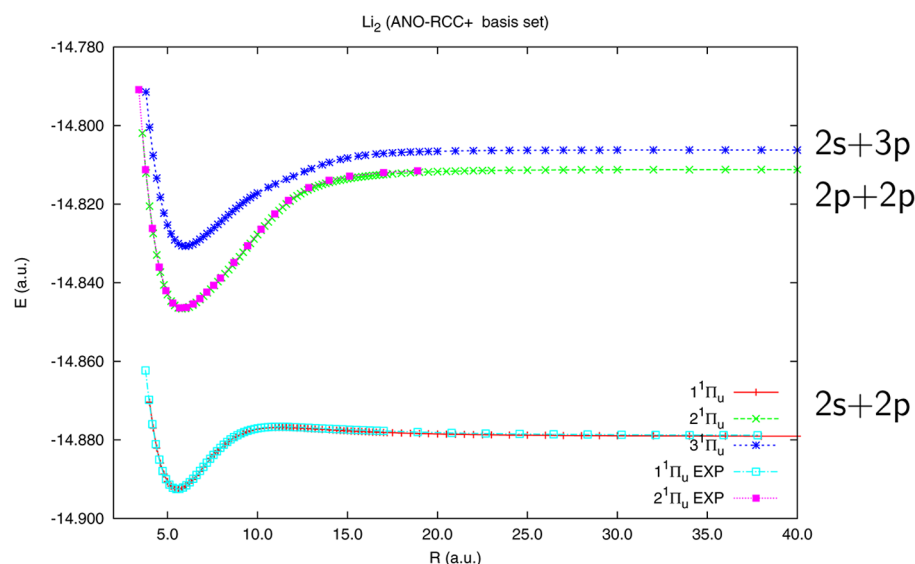


Figure 9. Potential energy curves for the Li_2 molecule with the FS-CCSD(2,0) method for the $1\Pi_u$ states in the ANO-RCC+ basis set. Experimental curves from refs 28 and 29.

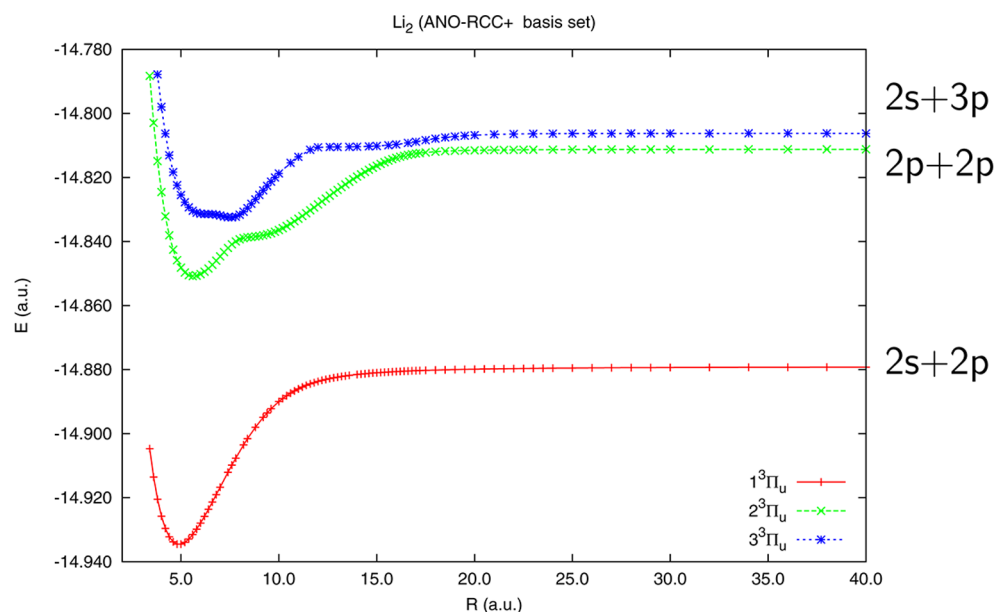


Figure 10. Potential energy curves for the Li_2 molecule with the FS-CCSD(2,0) method for the $3\Pi_u$ states in the ANO-RCC+ basis set.

should note, however, that the other theoretical values^{40,41} stay also close to 3.85 Å. An excellent agreement is observed also for the harmonic frequency with the maximum error of 2 wavenumbers. The adiabatic excitation energy is off the experiment by less than 0.01 eV for all four states for which experimental values are available with MAE of 0.006 eV. The similar average error is observed for the dissociation energy with the error of 1 to 31 cm^{-1} and the respective MAE value is significantly smaller for the current results (18 cm^{-1}) than for the other two theoretical works, cf. JS (174 cm^{-1})⁴⁰ and PS (96 cm^{-1}).⁴¹ In the latter works, this is due mostly to the poor result for the $1^1\Delta_g$ state: JS is off by 768 cm^{-1} , PS is off by 211 cm^{-1} , and the current work is off by 13 cm^{-1} .

For remaining electronic states for which the experimental data are not available, we observe in most cases a satisfactory agreement with other theoretical results. As an exception, we may quote $1^3\Delta_u$ state, which we find as bonding one with R_e equal to

3.121 Å, $D_e = 3902 \text{ cm}^{-1}$, $\omega_e = 255 \text{ cm}^{-1}$. These values are close to those by PS⁴¹ while in the calculations by JS⁴⁰ the state comes out as repulsive. The results obtained by Konowalow et al.⁴² indicate existence of the bond; however, some of our results are remarkably different; for example, D_e in this work, PS,⁴¹ and Konowalow et al.⁴² are equal to 3902, 3430, and 779, respectively.

For the electronic states belonging to the group correlating to the $2s + 3p$ asymptote (see Table 7), we have found experimental data only for the two states ($3^3\Sigma_g^+$, $6^1\Sigma_g^+$) and that is why we confront our results with those by PS who report in⁴¹ values for all eight states; two of them ($3^3\Sigma_g^+$ and $3^3\Sigma_u^+$) were also reported in the works by JS⁴⁰ and Schmidt-Mink et al.⁴³ According to our findings, the six states belonging to this group reveal a double-well character and the two ($3^1\Pi_u$ and $3^3\Pi_u$) have a single minimum. In several cases, our results are very close to those obtained by other theoretical works. The $3^3\Sigma_g^+$ state is an

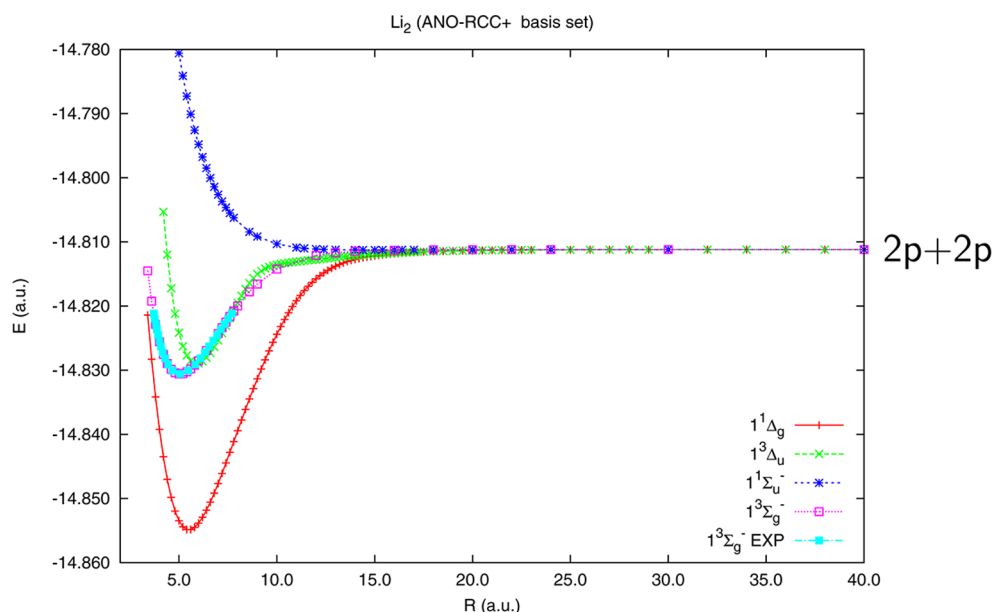


Figure 11. Potential energy curves for the Li_2 molecule with the FS-CCSD(2,0) method for the $1^1\Delta_g$, $1^3\Delta_u$, $1^1\Sigma_u^-$, and $1^3\Sigma_g^-$ states in the ANO-RCC+ basis set. Experimental curve from ref 8.

Table 3. Spectroscopic Constants for Li_2 Molecule (FS-CCSD (2,0) Method, ANO-RCC+ Basis Set) $2s + 2s$ Dissociation Limit

sym.	R_e (Å)	D_e (cm^{-1})	ω_e (cm^{-1})	T_e (eV)
$X^1\Sigma_g^+$	2.677	8466	351	
expt. ^{27,30}	2.673	8517	351	
JS ^a	2.658	8613	352	
PS ^b	2.660	8510	353	
$1^3\Sigma_u^+$	4.169	334	65	1.008
expt. ^{17,23}	4.171	333	65	1.014
JS ^a	4.134	344	66	1.008
PS ^b	4.159	321	66	1.015
MAE _{present work} ^c	0.003	26	0	0.006
MAE _{JS} ^c	0.026	54	1	0.006
MAE _{PS} ^c	0.013	10	2	0.001

^aRef 40. ^bRef 41. ^cMean absolute error.

example where the current results agree very well with those obtained in papers.^{40,41,43} For example, the harmonic frequency of JS,⁴⁰ PS⁴¹ is identical to ours with the difference of 5 cm^{-1} to that by Schmidt-Mink et al.⁴³ In some cases, we observe larger differences; for example, in $6^3\Sigma_u^+$, our results differ from those by PS by ca. 0.5 Å in R_e , by ca. 2300 cm^{-1} in D_e (2798 vs 519 cm^{-1}), and 35 cm^{-1} in harmonic frequency.

4.2. Electronic States with Double Minima. The lowest energy double well states occur in the group correlating with the $2s + 3s$ asymptote. We have there a well-known $2^1\Sigma_u^+$ state with two distinct minima separated by the barrier, see Figure 5. The minima occur at the 3.093 and 6.088 Å and with the energy difference of 219 cm^{-1} and the barrier height equal to 2167 cm^{-1} .

The double well phenomenon is much more frequently observed in the higher lying electronic states. For example, the typical shape of the PEC for the higher singlet Σ_g^+ states is a relatively deep first minimum seen around $3.0\text{--}3.5 \text{ Å}$ and the shelf occurring at larger distance, which, according to our calculations, turns out to be a very shallow minimum of the depth of the few wavenumbers. This can be observed for $3^1\Sigma_g^+$ ($2s + 3s$), and the same pattern is also observed for the $4^1\Sigma_g^+$ ($2p + 2p$),

Table 4. Spectroscopic Constants for Li_2 Molecule (FS-CCSD (2,0) Method, ANO-RCC+ basis set) $2s + 2p$ Dissociation Limit

sym.	R_e (Å)	D_e (cm^{-1})	ω_e (cm^{-1})	T_e (eV)
$1^3\Pi_u$	2.592	12166	346	1.390
expt. ²⁵	2.590	12145	346	
JS ^a	2.577	12297	348	1.392
PS ^b	2.581	12178	349	1.393
$1^1\Sigma_u^+$	3.112	9356	255	1.739
expt. ³³	3.108	9353	257	1.744
JS ^a	3.092	9483	258	1.735
PS ^b	3.094	9466	257	1.729
$1^3\Sigma_g^+$	3.071	7080	251	2.021
expt. ²³	3.068	7092	251	2.024
JS ^a	3.053	7184	253	2.020
PS ^b	3.055	7137	253	2.018
$1^1\Pi_u$	2.942	2930	270	2.536
expt. ³⁰	2.936	2984	271	2.534
JS ^a	2.934	2930	269	2.548
PS ^b	2.939	2716	270	2.566
$2^1\Sigma_g^+$	3.655	3289	128	2.491
expt. ³⁴	3.651	3319	129	2.492
JS ^a	3.655	3274	130	2.497
PS ^b	3.667	3161	126	2.511
$1^1\Pi_g$	4.061	1426	93	2.722
expt. ⁹	4.058	1423	93	2.726
JS ^a	4.048	1426	93	2.724
PS ^b	4.063	1400	93	2.729
$1^3\Pi_g$	repulsive			
$2^3\Sigma_u^+$	3.194	−5658	215	3.605
expt.				
JS ^a	3.181	−5669	194	
PS ^b	3.185	−5712	213	
MAE _{present work} ^c	0.004	21	1	0.003
MAE _{JS} ^c	0.010	79	1	0.007
MAE _{PS} ^c	0.010	107	2	0.015

^aRef 40. ^bRef 41. ^cMean absolute error.

Table 5. Spectroscopic Constants for Li₂ Molecule (FS-CCSD (2,0) method, ANO-RCC+ basis set) 2s + 3s dissociation limit

sym.	R _e (Å)	D _e (cm ⁻¹)	ω _e (cm ⁻¹)	T _e (eV)
3 ¹ Σ _g ⁺ inner	3.089	8290	248	3.392
expt. ¹⁸	3.086	8313	246	3.398
JS ^a	3.076	8333	247	3.401
PS ^b	3.074	8289	250	3.401
3 ¹ Σ _g ⁺ outer	5.740	5795		3.702
expt. ³	5.760			
2 ³ Σ _g ⁺	3.084	8410	269	3.378
expt. ¹⁵	3.080		269	3.384
JS ^a	3.073	8451	270	3.388
PS ^b	3.075	8428	270	3.384
2 ¹ Σ _u ⁺ inner	3.093	5608	260	3.725
expt. ^{14,29}	3.094	5615	260	3.732
JS ^a	3.081	5674	260	3.731
PS ^b	3.083	5660	260	3.727
2 ¹ Σ _u ⁺ outer	6.088	5389	118	3.752
expt. ^{14,29}	6.040	5321		3.769
JS ^a	6.072	5413	119	3.755
PS ^b	6.080	5453	117	3.753
3 ³ Σ _u ⁺	3.658	5879	350	3.691
expt.				
JS ^a	3.658	5903	373	3.710
PS ^b	3.667	5866	356	3.701
MAE _{present work} ^c	0.015	33	1	0.009
MAE _{JS} ^c	0.016	57	1	0.006
MAE _{PS} ^c	0.017	67	2	0.006

^aRef 40. ^bRef 41. ^cMean absolute error.

5¹Σ_g⁺ (2p + 2p), 6¹Σ_g⁺ (2s + 3p) (dissociation limit in parentheses). A better shaped minima can be seen for the 3³Σ_g⁺ curve (2s + 3p) where the second one is 78 cm⁻¹ deep. The triplet state curve manifesting two minima is that of 6³Σ_u⁺ with the first one occurring at 3.180 Å and the second one occurring at 9.490 Å. Here, the first minimum—relatively deep—occurs at the 3.089 Å with the barrier of 2498 cm⁻¹ while the second corresponds to the 5.740 Å with the depth of the 4 cm⁻¹. The existence of the second minimum has been confirmed experimentally by Jastrzębski et al.³ whereas the other theoretical work pointing to its presence is that by Konowalow et al.⁴²

5. CONCLUSIONS

A systematic theoretical study devoted to the calculation of the potential energy curves and selected spectroscopic constants for 34 electronic states of the Li₂ molecule is presented. This work is an example of the successful application of the method belonging to the coupled cluster family in the high accuracy spectroscopy. We point out the overall excellent agreement of the results obtained in this work with the experimental data. The computed PECs perfectly overlap with the RKR or IPA curves whenever they are available; in Figures 2–11, we have compared 18 experimental curves with those obtained in this work. Similarly, a very good agreement is observed for the examples for which the experimental curves display either a double-well or shelf character. The same is true for the spectroscopic constants presented in Tables 3–7. In most cases, the difference between the computed and experimental equilibrium distance, R_e, is less than 0.004 Å, and only in 2 out of 18 cases is it of the order of 0.01 Å. The mean absolute error for the R_e evaluated for the 18 states is equal to 0.005 Å, which is a better result than in other theoretical studies including those obtained with the FCI scheme

Table 6. Spectroscopic Constants for Li₂ Molecule (FS-CCSD (2,0) Method, ANO-RCC+ Basis Set) 2p + 2p Dissociation Limit

sym.	R _e (Å)	D _e (cm ⁻¹)	ω _e (cm ⁻¹)	T _e (eV)
4 ¹ Σ _g ⁺ inner	3.547	8380	225	3.709
expt. ¹⁹	3.548	8349	227	3.716
JS ^a	3.545	8388	229	3.718
PS ^b	3.543	8377	231	3.712
4 ¹ Σ _g ⁺ outer	9.020	2197	24	4.476
expt. ⁴	9.010			
JS ^a	9.107	2159	19	4.477
PS ^b	8.750	2158	17	4.483
4 ³ Σ _u ⁺	3.248	4538	209	4.185
expt.				
JS ^a	3.351	4157	187	4.240
PS ^b	3.267	4395	206	4.206
5 ³ Σ _u ⁺	3.145	3428	258	4.323
expt.				
JS ^a	3.149	3260	265	4.356
PS ^b	3.126	3079	265	4.369
2 ¹ Π _g	3.201	6481	230	3.944
expt. ¹⁰	3.201	6455	230	3.951
JS ^a	3.191	6469	231	3.956
PS ^b	3.201	6398	229	3.958
2 ³ Π _g	3.851	8505	187	3.693
expt. ²⁰	3.816	8484	189	3.700
JS ^a	3.853	8511	190	3.700
PS ^b	3.851	8435	191	3.705
2 ¹ Π _u	3.086	7773	237	3.784
expt. ^{29,31}	3.081	7774	239	3.788
JS ^a	3.077	7751	236	3.797
PS ^b	3.089	7641	231	3.803
2 ³ Π _u	2.980	8696	283	3.670
expt.				
JS ^a	2.968	8720	284	3.680
PS ^b	2.965	8671	284	3.676
1 ¹ Δ _g	2.913	9592	274	3.559
expt. ²⁶		9579	271	
JS ^a	2.822	8811	276	3.668
PS ^b	2.919	9368	273	3.589
1 ³ Δ _u	3.121	3902	255	4.264
expt.				
JS ^a	repulsive			
PS ^b	3.126	3430	252	4.326
5 ¹ Σ _g ⁺ inner	3.215	5010	248	4.127
expt. ⁵	3.220			4.131
PS ^b	3.267	4545	258	4.187
5 ¹ Σ _g ⁺ outer	4.879	2532	51	4.434
expt.				
PS ^b	4.660	2423	82	4.450
1 ¹ Σ _u ⁻	7.648	14	10	4.746
expt.				
PS ^b	repulsive			
1 ³ Σ _g ⁻	2.671	4259	217	4.220
expt.				
PS ^b	2.682	4032	218	4.251
MAE _{present work} ^c	0.024	18	2	0.006
MAE _{JS} ^c	0.030	174	2	0.004
MAE _{PS} ^c	0.059	96	3	0.017

^aRef 40. ^bRef 41. ^cMean absolute error.

Table 7. Spectroscopic Constants for Li₂ Molecule (FS-CCSD (2,0) Method, ANO-RCC+ Basis Set) 2s + 3p Dissociation Limit

sym.	$R_e(\text{\AA})$	$D_e(\text{cm}^{-1})$	$\omega_e(\text{cm}^{-1})$	$T_e(\text{eV})$
$3^3\Sigma_g^+$ inner	3.046	8389	274	3.843
expt. ¹⁵	3.038			3.849
JS ^a	3.034	8446	274	3.851
PS ^b	3.034	8346	274	3.855
$3^3\Sigma_g^+$ outer	6.310	1926	105	4.645
expt.				
PS ^b	6.280	1852	106	4.660
$3^1\Sigma_u^+$ inner	3.250	5628	193	4.186
expt.				
PS ^b	3.292	5495	176	4.208
$3^1\Sigma_u^+$ outer	4.360	5874	306	4.155
expt.				
JS ^a	4.369	5848	295	4.174
PS ^b	4.340	5839	258	4.165
$6^3\Sigma_g^+$ inner	3.172	5151	264	4.245
expt. ^{5,21}	3.176			4.252
PS ^b	3.129	3008	230	4.517
$6^1\Sigma_g^+$ outer	13.598	1084	68	4.749
expt.				
PS ^b	4.010	2513	106	4.573
$6^3\Sigma_u^+$ inner	3.180	2798	234	4.537
expt.				
PS ^b	3.670	519	199	4.825
$6^3\Sigma_u^+$ outer	9.490	375	36	4.837
expt.				
PS ^b	4.700	165	156	4.869
$3^1\Pi_g$ inner	3.188	4075	228	4.378
expt.				
PS ^b	3.359	2803	187	4.542
$3^1\Pi_g$ outer	8.540	89	18	4.873
expt.				
PS ^b	8.170	65	16	4.882
$3^3\Pi_g$ inner	3.134	6050	254	4.133
expt.				
PS ^b	3.139	5727	253	4.179
$3^3\Pi_g$ outer	7.310	571	31	4.813
expt.				
PS ^b	6.700	547	38	4.822
$3^1\Pi_u$	3.170	5376	236	4.217
expt.				
PS ^b	3.184	5084	230	4.259
$3^3\Pi_u$ inner	3.970	5748	198	4.171
expt.				
PS ^b	3.979	5645	231	4.190
MAE _{present work} ^c	0.006			0.007
MAE _{JS} ^c	0.004			0.002
MAE _{PS} ^c	0.026			0.136

^aRef 40. ^bRef 41. ^cMean absolute error.

based on the model or effective potentials. Similarly, for the dissociation energy, D_e , the MAE value for the 15 states for which experimental data are available is 20 cm^{-1} , while the MAE for the harmonic frequencies is only 0.94 cm^{-1} (16 states). The same excellent agreement is observed for excitation energy, T_e , for which an average error is 0.005 eV (computed for 16 states). In the evaluation of the MAEs for the spectroscopic constants, we have considered only the inner minima for the double-well curves.

We may conclude that the recently introduced FS-CCSD-(2,0)⁵⁹ approach is a convenient computational scheme to describe the dissociation of the single bond. The Hartree–Fock calculations for the Li₂⁺ ion we obtain a smooth curve for all interatomic distances due to the fact that the latter ion dissociates into the closed shell fragments (Li⁺ ions). By applying then the FS-CCSD(2,0) scheme designed to recover the double electron attached states we end up with the accurate description of the electronic states for the neutral Li₂ molecule.

The same computational scheme has been recently employed in the generation of the potential energy curves used in the study of the photoassociation of the Rb₂ molecule from the ultracold atoms.⁶⁸

AUTHOR INFORMATION

Corresponding Author

*E-mail: musial@ich.us.edu.pl.

Notes

The authors declare no competing financial interest.

ACKNOWLEDGMENTS

This work has been supported by the National Science Centre, Poland under Grant No. 2011/01/B/ST4/06503.

REFERENCES

- (1) He, Ch.; Gold, L. P.; Bernheim, R. A. *J. Chem. Phys.* **1991**, *95*, 7947–7951.
- (2) Bernheim, R. A.; Gold, L. P.; Tomczyk, C. A.; Vidal, C. R. *J. Chem. Phys.* **1987**, *87*, 861–868.
- (3) Jastrzebski, W.; Pashov, A.; Kowalczyk, P. *J. Chem. Phys.* **2001**, *114*, 10725–10727.
- (4) Pashov, A.; Jastrzebski, W.; Kowalczyk, P. *J. Chem. Phys.* **2000**, *113*, 6624–6628.
- (5) Song, M.; Yi, P.; Dai, X.; Liu, Y.; Li, L.; Jeung, G.-H. *J. Mol. Spectrosc.* **2002**, *215*, 251–261.
- (6) Lazarov, G.; Lyyra, A. M.; Li, L. *J. Mol. Spectrosc.* **2001**, *205*, 73–80.
- (7) Li, D.; Xie, F.; Li, L.; Lazoudis, A.; Lyyra, A. M. *J. Mol. Spectrosc.* **2007**, *246*, 180–186.
- (8) Yiannopoulou, A.; Ji, B.; Li, L.; Li, M.; Urbanski, K.; Lyyra, A. M.; Stwalley, W. C.; Jeung, G.-H. *J. Chem. Phys.* **1994**, *101*, 3581–3587.
- (9) Miller, D. A.; Gold, L. P.; Tripodi, P. D.; Bernheim, R. A. *J. Chem. Phys.* **1990**, *92*, 5822–5825.
- (10) Bernheim, R. A.; Gold, L. P.; Kelly, P. B.; Tipton, T.; Veirs, D. K. *J. Chem. Phys.* **1981**, *74*, 2749–2754.
- (11) Linton, C.; Martin, F.; Ross, A. J.; Russier, I.; Crozet, P.; Yiannopoulou, A.; Li, L.; Lyyra, A. M. *J. Mol. Spectrosc.* **1999**, *196*, 20–28.
- (12) Qi, P.; Lazarov, G.; Lyyra, A. M.; Jeung, G.-H. *J. Mol. Spectrosc.* **2008**, *247*, 184–186.
- (13) Antonova, A.; Lazarov, G.; Urbanski, K.; Lyyra, A. M.; Li, L.; Jeung, G.-H.; Stwalley, W. C. *J. Chem. Phys.* **2000**, *112*, 7080–7088.
- (14) Kasahara, S.; Kowalczyk, P.; Kabir, Md. H.; Baba, M.; Katô, H. *J. Chem. Phys.* **2000**, *113*, 6227–6234.
- (15) Yiannopoulou, Y.; Urbanski, K.; Lyyra, A. M.; Li, L.; Ji, B.; Bahns, J. T.; Stwalley, W. C. *J. Chem. Phys.* **1995**, *102*, 3024–3031.
- (16) Ross, A. J.; Crozet, P.; Linton, C.; Martin, F.; Russier, I.; Yiannopoulou, A. *J. Mol. Spectrosc.* **1998**, *191*, 28–31.
- (17) Xie, X.; Field, R. W. *J. Chem. Phys.* **1985**, *83*, 6193–6196.
- (18) Bernheim, R. A.; Gold, L. P.; Kelly, P. B.; Tipton, T.; Veirs, D. K. *J. Chem. Phys.* **1982**, *76*, 57–60.
- (19) Bernheim, R. A.; Gold, L. P.; Kelly, P. B.; Tomczyk, C.; Veirs, D. K. *J. Chem. Phys.* **1981**, *74*, 3249–3254.
- (20) Xie, X.; Field, R. W. *J. Mol. Spectrosc.* **1986**, *117*, 228–244.
- (21) Bernheim, R.; Gold, L. P.; Tipton, T. *J. Chem. Phys.* **1983**, *78*, 3635–3646.

- (22) Urbanski, K.; Antonova, S.; Yiannopoulou, A.; Lyyra, M.; Li, L.; Stwalley, W. C. *J. Chem. Phys.* **1996**, *104*, 2813–2817.
- (23) Linton, C.; Murphy, T. L.; Martin, F.; Barcis, R.; Verges, J. *J. Chem. Phys.* **1989**, *91*, 6036–6041.
- (24) Linton, C.; Martin, F.; Bacis, R.; Verges, J. *J. Mol. Spectrosc.* **1989**, *137*, 235–241.
- (25) Engelke, F.; Hage, H. *Chem. Phys. Lett.* **1983**, *103*, 98–102.
- (26) Linton, C.; Martin, F.; Crozet, P.; Roos, A. J.; Bacis, R. *J. Mol. Spectrosc.* **1993**, *158*, 445–454.
- (27) Barakat, B.; Bacis, R.; ACarrot, F.; Churassy, S.; Crozet, P.; Martin, F.; Verges, J. *J. Chem. Phys.* **1986**, *102*, 215–227.
- (28) Bouloufa, N.; Cacciani, P.; Vetter, R.; Yiannopoulou, A.; Martin, F.; Ross, A. J. *J. Chem. Phys.* **2001**, *114*, 8445–8458.
- (29) Kubkowska, M. K.; Grochola, A.; Jastrzebski, W.; Kowalczyk, P. *Chem. Phys.* **2007**, *333*, 214–218.
- (30) Hessel, M. M.; Vidal, C. R. *J. Chem. Phys.* **1979**, *70*, 4439–4459.
- (31) Ishikawa, K.; Kubo, S.; Kato, H. *J. Chem. Phys.* **1991**, *95*, 8803–8808.
- (32) Jedrzejewski-Szmek, Z.; Grochola, A.; Jastrzebski, W.; Kowalczyk, P. *Chem. Phys. Lett.* **2007**, *444*, 229–231.
- (33) Kusch, P.; Hessel, M. M. *J. Chem. Phys.* **1977**, *67*, 586–589.
- (34) Barakat, B.; Bacis, R.; Churassy, S.; Field, R. W.; Ho, J.; Linton, C.; McDonald, S.; Martin, F.; Verges, J. *J. Mol. Spectrosc.* **1986**, *116*, 271–285.
- (35) Jedrzejewski-Szmek, Z.; Grochola, A.; Jastrzebski, W.; Kowalczyk, P. *Opt. Applicata* **2010**, *40*, 577–585.
- (36) Adohi-Krou, A.; Martin, F.; Ross, A. J.; Linton, C.; Le Roy, R. J. *J. Chem. Phys.* **2004**, *121*, 6309–6316.
- (37) Wang, X.; Magnes, J.; Lyyra, A. M.; Ross, A. J.; Martin, F.; Dove, P. M.; Le Roy, R. J. *J. Chem. Phys.* **2002**, *117*, 9339–9346.
- (38) Le Roy, R. J.; Dattani, N. S.; Coxon, J. A.; Ross, A. J.; Crozet, P.; Linton, C. *J. Chem. Phys.* **2009**, *131*, 204309–1–17.
- (39) Shi, D.-H.; Ma, H.; Sun, J.-F.; Zhu, Z.-L. *Commun. Theor. Phys.* **2007**, *47*, 1114–1120.
- (40) Jasik, P.; Sienkiewicz, J. E. *Chem. Phys.* **2006**, *323*, 563–573.
- (41) Poteau, R.; Spiegelmann, F. *J. Mol. Spectrosc.* **1995**, *171*, 299–308.
- (42) Konowalow, D. D.; Fish, J. L. *Chem. Phys.* **1984**, *84*, 463–475.
- (43) Schmidt-Mink, I.; Müller, W.; Meyer, W. *Chem. Phys.* **1985**, *92*, 263–285.
- (44) Müller, W.; Meyer, W. *J. Chem. Phys.* **1984**, *80*, 3311–3320.
- (45) Minaev, B. *Spectrochim. Acta A* **2005**, *62*, 790–799.
- (46) Konowalow, D. D.; Olson, M. L. *J. Chem. Phys.* **1979**, *71*, 450–457.
- (47) Kaldor, U. *Chem. Phys.* **1990**, *140*, 1–6.
- (48) Musiał, M.; Kowalska-Szajda, K.; Lyakh, D. I.; Bartlett, R. J. *J. Chem. Phys.* **2013**, *138*, 194103–1–8.
- (49) Shi, D.-H.; Ma, H.; Sun, J.-F.; Zhu, Z.-L. *Commun. Theor. Phys.* **2007**, *48*, 1081–1087.
- (50) Shi, D.-H.; Sun, J.-F.; Zhu, Z.-L.; Liu, Y.-F. *Chin. Phys.* **2007**, *16*, 2701–2708.
- (51) Shi, D.-H.; Ma, H.; Sun, J.-F.; Zhu, Z.-L.; Liu, Y.-F.; Yu, B.-H. *J. Mol. Struct. (THEOCHEM)* **2007**, *824*, 71–75.
- (52) Yu, B.-H.; Shi, D.-H.; Sun, J.-F.; Zhu, Z.-L.; Liu, Y.-F.; Yang, X.-D. *Chin. Phys.* **2007**, *16*, 2371–2377.
- (53) Liu, Y.-F.; Sun, J.-F.; Ma, H.; Zhu, Z.-L. *Chin. Phys.* **2007**, *16*, 680–685.
- (54) Nakatsuji, H.; Ushio, J.; Yonezawa, T. *Can. J. Chem.* **1985**, *63*, 1857–1863.
- (55) Jeung, G. H. *J. Phys. B, At. Mol. Phys.* **1983**, *16*, 4289–4297.
- (56) Henriët, A.; Masnou-Seeuws, F. *J. Phys. B* **1988**, *21*, 339–346.
- (57) Lyakh, D. I.; Musiał, M.; Lotrich, V.; Bartlett, R. J. *Chem. Rev.* **2012**, *112*, 182–243.
- (58) Bartlett, R. J.; Musiał, M. *Rev. Mod. Phys.* **2007**, *79*, 291–352.
- (59) Musiał, M. *J. Chem. Phys.* **2012**, *136*, 134111–1–14.
- (60) Mieszczanin, P.; Musiał, M.; Kucharski, S. A. *Mol. Phys.* **2013**, DOI: dx.doi.org/10.1080/00268976.2013.856488.
- (61) Musiał, M.; Bartlett, R. J. *J. Chem. Phys.* **2004**, *121*, 1670–1675.
- (62) Musiał, M.; Bartlett, R. J. *J. Chem. Phys.* **2003**, *119*, 1901–1908.
- (63) Meissner, L. *J. Chem. Phys.* **1998**, *108*, 9227–9235.
- (64) Musiał, M.; Bartlett, R. J. *J. Chem. Phys.* **2008**, *129*, 134105–1–12.
- (65) ACES II program is a product of the Quantum Theory Project, University of Florida Authors: Stanton, J. F.; Gauss, J.; Watts, J. D.; Nooijen, M.; Oliphant, N.; Perera, S. A.; Szalay, P. G.; Lauderdale, W. J.; Kucharski, S. A.; Gwaltney, S. R.; Beck, S.; Balková, A.; Musiał, M.; Bernholdt, D. E.; Baeck, K.-K.; Sekino, H.; Rozyczko, P.; Huber, C.; Bartlett, R. J. Integral packages included are VMOL (Almlöf, J.; Taylor, P.); VPROPS (Taylor, P. R.). A modified version of ABACUS integral derivative package (Helgaker, T. U.; Jensen, H. J. Aa.; Olsen, J.; Jørgensen, P.; Taylor, P. R.).
- (66) Roos, O.; Veryazov, V.; Widmark, P.-O. *Theor. Chem. Acc.* **2003**, *111*, 345–351.
- (67) Le Roy, R. J. *LEVEL 8.0: A Computer Program for Solving the Radial Schrödinger Equation for Bound and Quasibound Levels*, Chemical Physics Research Report 2007; University of Waterloo: Waterloo, 2007; CP-663; <http://leroy.uwaterloo.ca/programs/>.
- (68) Tomza, M.; Goerz, M. H.; Musiał, M.; Moszynski, R.; Koch, Ch. *P. Phys. Rev. A* **2012**, *86*, 043424–1–13.
- (69) Radziemski, L. J.; Engleman, R., Jr.; Brault, J. W. *Phys. Rev. A* **1995**, *52*, 4462–4470.